



Curcumin-functionalized nanocomposite AgNPs/SDS/MWCNTs for electrocatalytic simultaneous determination of dopamine, uric acid, and guanine in co-existence of ascorbic acid by glassy carbon electrode

Negar Haghnegahdar¹, Maryam Abbasi Tarighat^{1,*} , and Davoud Dastan²

¹Department of Chemistry, Faculty of Sciences, Persian Gulf University, 75169 Bushehr, Iran

²School of Materials Science and Engineering, Georgia Institute of Technology, Atlanta, GA 30332, USA

Received: 30 September 2020

Accepted: 7 January 2021

Published online:

1 February 2021

© The Author(s), under exclusive licence to Springer Science+Business Media, LLC part of Springer Nature 2021

ABSTRACT

The binding of curcumin on the surface of AgNPs-sodium dodecyl sulfate (SDS)-multi-walled carbon nanotubes-glassy carbon electrode (CM/AgNPs/SDS/MWCNTs) was reported for simultaneous electrochemical determination of dopamine (DA), uric acid (UA) and guanine (GU). Morphological properties of modified electrodes surfaces were characterized using different voltammetry methods. The microscopic area of the modified electrode was obtained 0.139 cm^{-2} using chronoamperometry analysis. The scanning electron microscope (SEM), XRD, and TEM were used to monitor the sensor fabrication. The zeta potential results showed that SDS dispersed the pure AgNPs, and the AgNPs were significantly stabilized. Also, the results showed that the constructed CM-functionalized nanocomposite create a large surface area, long stability, good adaptability, anti-interference capability, and significant reproducibility. The electrochemical results confirmed that the fabricated nanocomposite has a high electrocatalytic activity toward the oxidation of analytes especially for DA (vs. Ag/AgCl). While the above results hold true for DA, UA, and guanine GU determination, there was no comparable electrochemical peak for ascorbic acid (AA). The calibration curves were linear in the range of 12.0–200.0, 16.0–400.0, and 18–650.0 $\mu\text{mol L}^{-1}$ for DA, GU, and UA, respectively. The detection limit values were 0.14 $\mu\text{mol L}^{-1}$ for DA, 0.19 $\mu\text{mol L}^{-1}$ for GU, and 0.38 $\mu\text{mol L}^{-1}$ for UA. The prepared electrode was applied successfully to the simultaneous determination of analytes in blood, serum, urine, and *dopadic* ampoule samples.

Address correspondence to E-mail: matarighat@pgu.ac.ir; matarighat@gmail.com

1 Introduction

In the complex human body fluids (e.g., serum), there exists are many of biological molecules such as GU, UA, DA, and AA. These molecules have a significant effect on human physiology and play a serious function in the efficiency of cardiovascular, central nervous, renal, and hormonal systems as variation in relative concentration affects human health. Therefore, it proves necessary to develop rapid, practical, selective, and sensitive methods for accurately identifying of these molecules for both investigations of their physiological impact and diagnoses of several diseases [1]. GU is the second-most common purine found in the nucleic acids and appearing in both DNA and RNA molecules. Not only the GU nucleotides are involved in intermediary metabolism, but they also found in many mammalian excrements and tissues.

The main product of purine metabolism is UA, which is present in blood and human urine. An unusual amount of UA may cause hyperuricaemia, gout, or Lesch–Nyan disease. Catecholamine DA is an important neurotransmitter that plays essential roles in the operation of the central nervous system of mammals. Unusually low concentrations of DA may cause serious health problems, such as schizophrenia, Parkinson's disease, epilepsy, or Alzheimer's disease [2, 3]. Ascorbic Acid (AA), as a vital vitamin, is suggested for inhibition and treatment of common cold, infertility, and mental illness. It should be noted that the UA, DA, GU, and AA have similar oxidation potentials at bare electrodes and produce overlapping signals. The great problem with DA detection regards low concentration levels of DA compared to AA and UA. As a result, the interference effect of AA occurs at 0.2–0.4 mM (excess of AA in extracellular fluids).

Oxidized DA causes catalytic oxidation of AA and causes major interference in the detection of DA. Thus, it is critical to recognize the DA signal from AA and UA signals and eliminate the interference effect of AA [4]. Also, their oxidation products may be absorbed or electropolymerized on the bare electrodes and change their reusability and reproducibility. Recently, experiments such as capillary electrophoresis [5], high-performance liquid chromatography [6], a spectrophotometric method [7], and electrochemical method [8] were introduced to

detect two or three components of UA, DA, and AA simultaneously, such as.

Among these processes, the electrochemical method for detecting UA, DA, and AA has attracted considerable attention due to its numerous advantages. The advantages include simplicity, sensitivity, relatively low cost, and fast response [9, 10].

The similar oxidation potentials of biological compounds and accumulation of oxidation products of them at the electrode surface are major problems that decrease reusability, selectivity, and reproducibility of electrodes. So, construction of selective, sensitive, and reusable electrodes are interested. Our literature review details different modified electrodes that have been fabricated and applied to overcome this problem. After the fabrication of the first carbon nanotubes (CNTs)-based electrochemical sensors, the CNTs have been considered to develop of electrochemical sensors [11, 12]. Carbon-based nanomaterials (Carbon nanotubes, graphene, and its derivatives) have been utilized in both modifications of glassy carbon electrode (GCE) and carbon paste electrode (CPE) for determination of target analytes. In this area, we discuss single-walled carbon nanotubes (SWCNTs) [12], MWCNTs [13], MWCNTs/metal nanoparticles (MNPs), [14, 15] carbon nanohorns [2], grapheme/MWCNTs [16], graphene, and its derivatives [17, 18].

Also, modification of electrode surface was performed by metal nanoparticles (MNPs) [19], composite of MNPs [2], hybrid of MWCNTs, and MNPs [20], and polymeric materials [21]. It is difficult to apply some of these techniques to quantize of targets in biological fluids due to decreasing sensitivity. Also, the detection limits of some of the reported methods are quite varied [22]. Silver nanoparticles (AgNPs) were used for fabrication of different sensors and biosensors. AgNPs have several advantages such as high catalytic activity, good conductivity, small dimensional size, effective mass transport, and biocompatibility [23].

Curcumin (1,7-bis[4-hydroxy-3-methoxyphenyl]-1,6-heptadiene-3,5-dione)(CM) is a principal pigment obtained from curcuma. Curcumin shows a wide background of biological activities such as antifungal [24], antibacterial [24], antidiabetic [25], anti-allergic [26], anti-cancer, anti-inflammatory [27], and anti-protozoal [28] activities. Based on prior knowledge, there are few reports of using CM in electrochemistry

methods for determinations or modification of electrode surface.

Curcumin was used to modify GCE for electrocatalytic determination of simple alcohols, glucose, and some amino acids. Also, CM multi-wall carbon nanotubes–glassy carbon electrode has been constructed to determine hydrazine [28]. On another note, surfactants are amphiphilic compounds that contain hydrophilic or hydrophobic moieties that can reduce surface tension or interfacial tension between molecules at the surface or interface. Since the surfactants can increase solubility, sensitivity, enrichment, anti-interference effect, and selectivity, these chemicals have been widely used in various fields of analytical chemistry. Recently, surfactants have been applied in electrochemical analysis for ion selective electrode and polarographic voltammetric analysis [29].

Previous studies show that the presence of cationic and anionic centers of the β -diketone structure of CM may affect the hydrophilic/hydrophobic balance between curcumin and sodium dodecyl sulfate (SDS). Therefore, the complex formation of CM and SDS will stabilize the β -diketone forms of CM [30].

In this work, we intended to use synergistic advantages of CM, SDS, Ag NPs, and MWCNTs to enhance the electron transfer between the GCE surface and therefore, improving the analytical performance of biological molecules determination. To the best of our knowledge, this is the first report on the application of CM for stabilization and functionalization of decorated MWCNTs/GCE by AgNPs for the simultaneous determination of DA, UA, and GU in the presence of ascorbic acid (AA). The results show that the adsorption of SDS on the electrode surface may enhance the solubility of CM in micellar media and significantly varying both the oxidation/reduction potential and transfer coefficients of analytes. As a result, they increase the rate of electron transfer and create large surface area respect to MWCNTs. By using the selective and sensitive constructed composite, simultaneous determination of DA, UA, and GU analyses was concluded done in multiple real samples without the interference of AA.

2 Experimental details

2.1 Reagents and materials

Multi-walled carbon nanotube (MWCNT) (outer diameter: 5–9 nm, inner diameter: 110–170 nm, purity: > 95%), Sodium dodecyl sulfate (SDS), uric acid, ascorbic acid, dopamine, adenine, and guanine were purchased from Sigma Aldrich. Sodium hydrogen phosphate, disodium hydrogen phosphate, sodium hydroxide, potassium chloride, potassium nitrate, hydrochloric acid, acetic acid, sodium acetate, sodium sulfate, sodium chloride, sodium carbonate, and ethanol were purchased from Merck (Darmstadt, Germany). pH adjustments were performed with 0.1 mol L⁻¹ HCl or NaOH solutions. Graphite powder, high purity Nujol oil, silver nitrate, poly (vinyl pyrrolidone) (PVP), and sodium borohydride (NaBH₄) were purchased from Fluka. CM (reference standard) was purchased (Beijing, China). The stock solution of CM (1.0 mM) was prepared with ethanol. The working solutions of CM were made through diluting the stock solution with pH 7.0 phosphate buffer (0.1 M). All Chemicals with analytical grade were used without further purification.

2.2 Apparatus

Electrochemical experiments were performed using the IM-6 impedance analyzer (IM6e from Zahner-Elektrik, Germany). The electrochemical cell was assembled with a conventional three-electrode system: CM/SDS/AgNPs/MWCNT/GCE was used as the working electrode. An Ag/AgCl and platinum wire were applied as the reference electrode and counter electrode, respectively. pH measurements were performed with a Metrohm model 713 pH/mV meter (Metrohm, Switzerland). The micrographs of the modified electrodes were investigated by scanning electron microscopy (SEM–EDX, XL30, Philips Netherland). Electron microscopy (TEM) image was obtained using Zeiss-EM10C at the accelerating voltage of 80 kV. The zeta potential of all dispersed AgNPs was estimated on Malvern Zetasizer Nano Series (Malvern, UK).

2.3 Synthesis of silver nanoparticles

AgNPs were synthesized using ice-cold sodium borohydride. First, 30 mL of 0.002 M sodium

borohydride (NaBH₄) solution and magnetic stir were added to an Erlenmeyer flask. The flask was placed in an ice bath on a stir plate (20 min). Then, 2 mL of 0.001 M silver nitrate solution (AgNO₃) was added into the stirring NaBH₄ solution at approximately 1 drop per second. The stirring was stopped as soon as all of the AgNO₃ is added. By mixing both solutions (i.e., NaBH₄ and AgNO₃), Ag ions were reduced and clustered to form nanoparticles [23].

2.4 Functionalization of nanocomposite (CM/AgNPs/SDS/MWCNT/GCE)

A bare GCE was polished with 0.3 μm Al₂O₃ powder and was rinsed with distilled water. Then, the sonication was subsequently performed for 10 min in a 1:1 solution of HNO₃ and distilled water. The cleaned GCE was electrochemically activated in a 1.0 mol L⁻¹ H₂SO₄ solution at a scan rate of 100 mV s⁻¹. In this study, highly dispersed MWCNTs were obtained by dispersing 1.0 mg MWCNTs in 5.0 mL 3:1:1 mixture of DDW, ethanol, and SDS under sonication for 30 min. To prepare MWCNT film at GCE (SDS/MWCNT/GCE), 10 μL of the black suspension of MWCNTs in SDS was directly placed on the cleaned electrode surface and then dried at room temperature (15 min). The CM/AgNPs/SDS/MWCNT/GCE, AgNPs/SDS/MWCNT/GCE, CM/SDS/MWCNT/GCE, and CM/GCE modified electrodes were prepared by coating the surface of GCE with 10 μL of CM/AgNPs/SDS/MWCNT suspension, AgNPs/SDS/MWCNT suspension, and CM solution, respectively. The electrodes were then dried for 15 min at room temperature before measurement. These took about 15 min to dry at the electrode surface.

2.5 Blood sample and urine sample preparation

Blood samples, taken from the blood transfusion Center, Bushehr, were transformed into EDTA anticoagulant tubes. Plasma samples were obtained after centrifugation at 1000 rpm for 10 min. The plasma samples were stored at - 80 °C until required, while urine was collected overnight. Then, 25 mL of urine sample was mixed with 1.0 mL of 1:1 H₂O: HNO₃ and was heated for 10 min. Next, the digested sample was filtered and diluted to the desired mark with distilled water [29].

3 Results and discussion

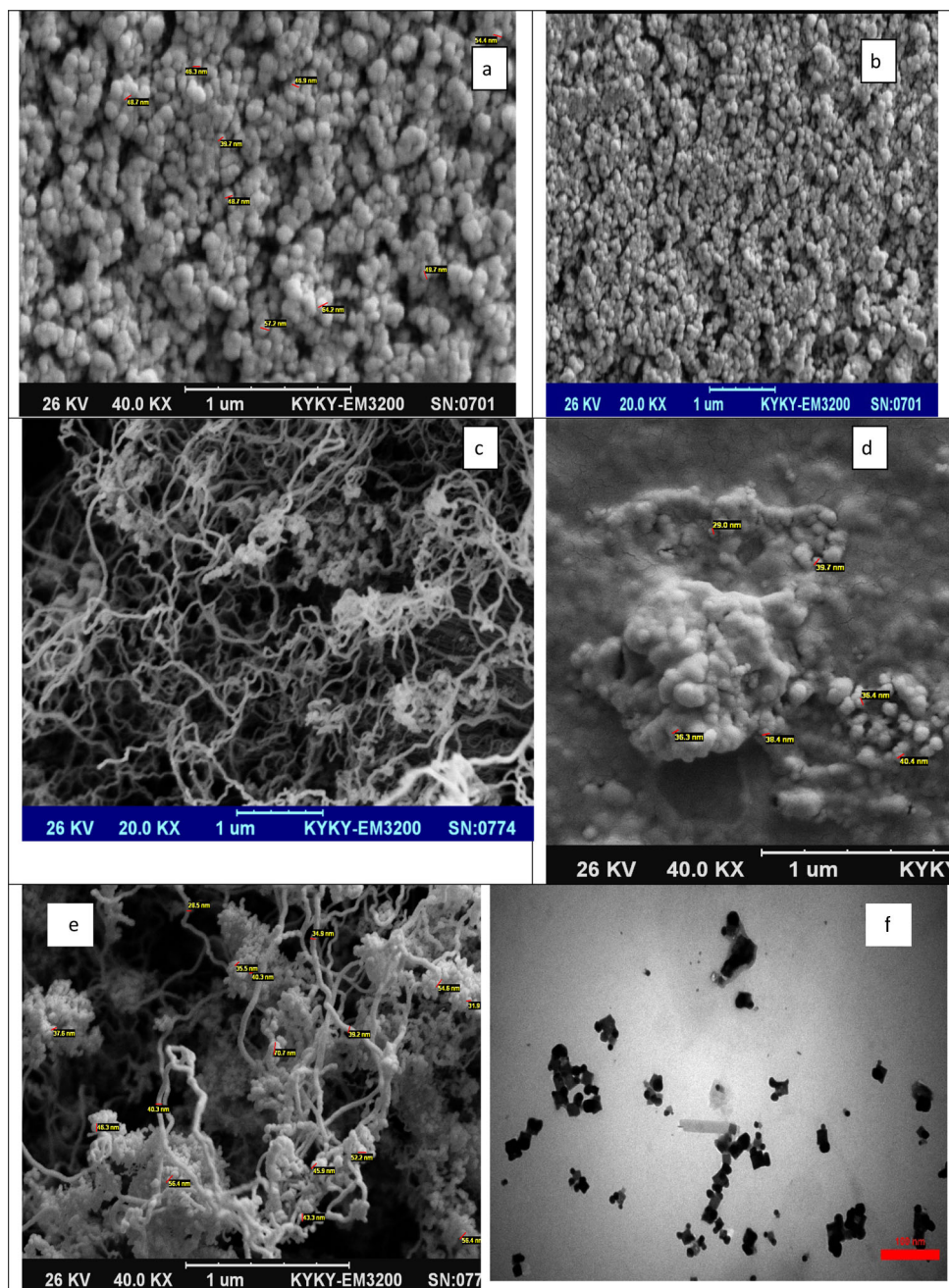
In this work, we tried to improve the solubility of CM without using an organic solvent. Also, we decided to use CM for modification, stabilization, and functionalization of decorated MWCNTs/GCE. SDS as an anionic surfactant at pH 7 can stabilize β-diketo form of CM where some of the medicinal effects of CM are connected with this tautomer. The absorption spectra of CM and CM-SDS were recorded. The results showed that in addition to the original band (425 nm), the new band at 350 nm has been introduced. The new band is due to the β-diketo tautomer of CM stabilized by CM and the SDS [30]. This tautomer has the maximum electron density in the structure of CM and combination of ion-dipole or H-bonding interaction results strong electron withdrawing or releasing effects [31].

3.1 Characterization of CM/AgNPs/SDS/MWCNT/GCE

The SEM image of the modified electrode is depicted in Fig. 1. Figure 1a shows that AgNPs formed a clear spherical structure with different sizes and heterogeneous dispersion. The dimensions of these nanoparticles differed with a diameter of about 39–64 nm, indicating an average particle size of 47.2 nm for Ag. Figure 1b and c portrays that the AgNPs and MWCNTs in SDS were immobilized on the GCE surface, which dispersed without aggregation, while MWCNTs maintained network-like structure. Figure 1c demonstrates that CM also stabilizes AgNPs. In this solution, the average size of silver nanoparticles was recorded as 35.6 nm. Figure 1d represents dispersion of MWCNT in SDS, and Fig. 1e shows the image of CM/AgNPs/SDS/MWCNT/GCE nanocomposite, implying that CM/AgNPs are distributed well on SDS/MWCNT/GCE surface. The random isolated distribution of CM/AgNPs/SDS-/MWCNTs increased the surface area of the sensor and could therefore result in high loading and fast response of analytes. TEM image of AgNPs is shown in Fig. 1f. The histogram for silver nanoparticles showed that the maximum particle size distribution was 39–64 nm, and average size of particles was 47 nm.

Also, the XRD patterns of composites structure are shown in Fig. 2. According this figure, the characteristic peaks were appeared at 12.0°, 17.1°, and 18.3°

Fig. 1 SEM image of modified electrode: **a** AgNPs, **b** AgNPs dispersed in SDS, **c** fictionalization of AgNPs with CM, **d** MWCNT dispersed in SDS, **e** CM/AgNPs/SDS/MWCNTs/GCE nanocomposite and **f** TEM image of AgNPs, respectively



for curcumin. XRD analysis of the MWCNT-Ag-CM nanocomposite reveals the characteristic peak at 28.4° owing to the presence of MWCNT and 38° , 45° , and 65° can be attributed to AgNPs in the composite. So, the results of XRD show that the composites were made of CM, Ag, and MWCNTs.

Moreover, the presence of AgNPs and CM on the MWCNTs surface are proved with observing the EDX analysis (Fig. 3). It can be proved with

observing the signals corresponding to C, O, and Ag in the EDX.

The zeta potential of bare AgNPs was compared with AgNPs zeta potential values dispersed in SDS to determine the stability. As expected, the surfactant changed the stability of the silver nanoparticles. Figure 4 illustrated, the bare AgNPs exhibited higher zeta potential than SDS-AgNPs. The zeta potential decreased upon changing pH from 2 to 8. The zeta potential of SDS-AgNPs is less than -30 mV,

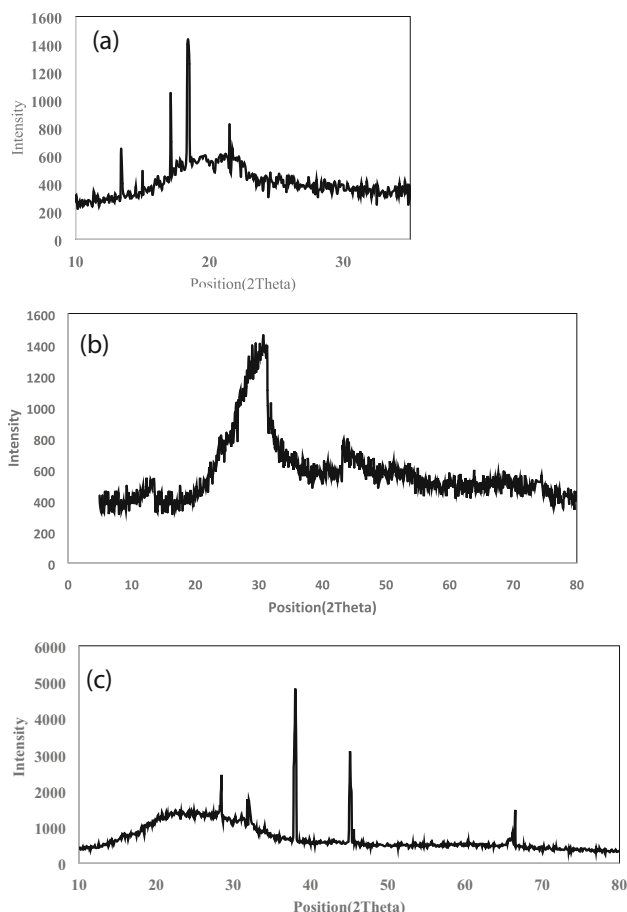


Fig. 2 XRD patterns of **a** CM, **b** MWCNT, and **c** MWCNT-CM-AgNPs

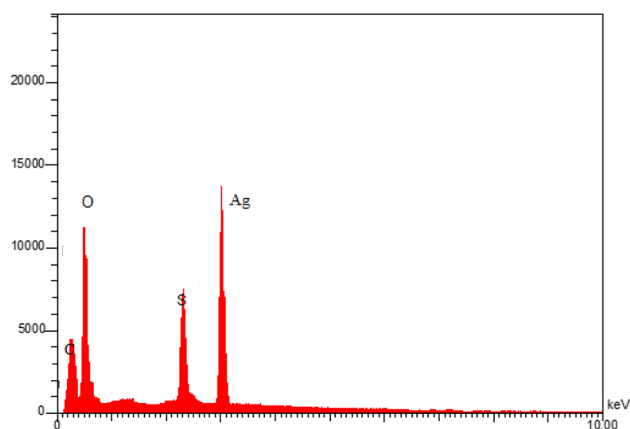


Fig. 3 Energy dispersive X-ray spectrum of fabricated nanocomposite

normally indicating strong stability. ESI was further applied for illustration of the differences between the electrochemical performance of bare GCE and modified GCE electrodes. Using a frequency response

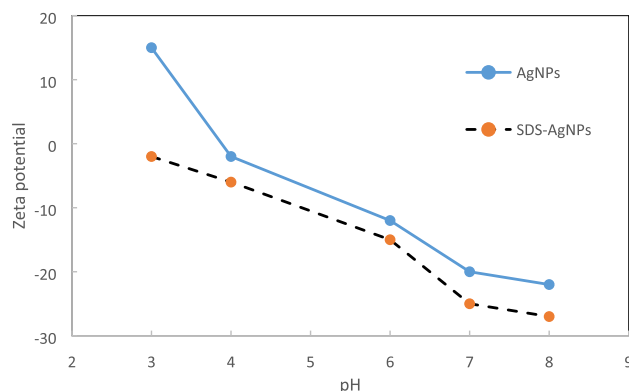


Fig. 4 Zeta potential of **a** bare AgNPs and **b** SDS-AgNPs as pH

analyzer (Nova1.7, The Netherlands), the data fittings and all simulations were performed.

The Nyquist plots of $1.0 \times 10^{-3} \text{ mol L}^{-1} \text{ K}_3[\text{Fe}(\text{CN})_6]$ in $0.1 \text{ mol L}^{-1} \text{ KCl}$ at pH 7 were recorded a frequency domain of 5 to 10 MHz. The plots showed a significant difference in bare GCE responses and the modified CM/AgNPs/SDS/MWCNT/GCE (Fig. 5). As can be conspicuously seen, the R_{ct} values were significantly decreased due to the excellent electrical conductivity of AgNPs and MWCNT after deposition of CM, SDS, AgNPs, and MWCNT on to the surface of GCE. This shows that synergistic effect of CM, AgNPs, and MWCNTs facilitated the electron transfer process on the electrode surface and further enhanced electrocatalytic effect of the fabricated electrode. Additionally, consideration of anodic and cathodic peak current of $\text{K}_3[\text{Fe}(\text{CN})_6]$ using functionalized nanocomposite showed notably separated and shifted peaks toward positive potentials. On average, both peak currents were 40 times greater than the bare electrode.

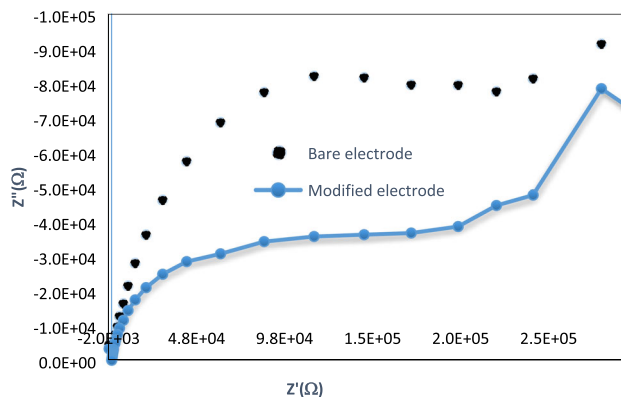


Fig. 5 The Nyquist plots of bare GCE and CM/SDS/AgNPs/MWCNT/GCE in KCl solution containing 1 mM $\text{Fe}(\text{CN})_6^{4-/3-}$

3.2 Electrochemistry of modified electrode

Cyclic voltammetry was utilized to explain the electrochemical behavior of different modifications of the electrode surface at pH 7. The electrochemical properties of DA ($5.0 \times 10^{-5} \text{ mol L}^{-1}$) using different electrodes were investigated. DA has an oxidation peak at 0.5 V at bare GCE. The CV values of different electrodes GCE, SDS/MWCNT/GCE, CM/GCE, and CM/AgNPs/SDS-MWCNT/GCE were recorded and are illustrated in Fig. 6. The peak current was magnified by 3.1, 22, 23, 29, and 40 times higher than bare GCE. These results show that the AgNPs and MWCNTs displayed superior electrical conductivity, interesting electrocatalytic activities, and great adsorption capacity of analytes. Furthermore, SDS enhanced the dispersion of the AgNPs and MWCNTs while CM improved the surface area. About biological molecules, the synergistic effect of CM, AgNPs, SDS, and MWCNTs can remarkably increase the sensitivity and selectivity of differential pulse voltammetry determination.

3.3 Optimization of experimental conditions

To reach the effective electroanalytical performance of the modified GCE, useful experimental variables such as pH, supporting electrolyte, amount of CM, and surfactant concentration were carefully studied and optimized in a solution containing $10 \mu\text{M}$ of targets. The DPV peaks of analytes were recorded, and DPV current changes were used for optimization of experimental parameters. The effect of buffer pH

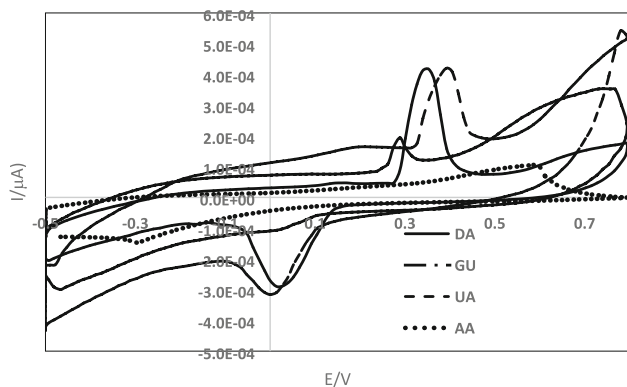


Fig. 6 CV of modified electrodes GCE, SDS/MWCNT/GCE, CM/GCE, and CM/AgNPs/SDS-MWCNT/GCE at optimum conditions

on the electro-oxidation of DA, UA, and GU was studied in the range of pH 4.0–8.0. Figure 7b illustrates that DPV currents were increased with increasing pH values. Therefore, a phosphate buffer of pH 7.0, which is compatible with the body's physical condition, was employed in further studies because the DPV current is more than other pHs values. As shown in Fig. 7a, the oxidation potentials of species were shifted positively when pH of solution decreases over the range 8.0 to 4.0. It is indicating that the electrochemical oxidation of analytes related to a proton-transfer process. The relationship of peak potential and pH is linear over the entire pH (7c). The regression equation was obtained $E(V) = 0.0521 \text{ pH} + 0.501$, $E(V) = 0.0499 \text{ pH} + 0.168$, and $E(V) = 0.0502 \text{ pH} + 0.577$ for Gu, UA, and DA, respectively (Fig. 7b and c). The linear slopes of the graphs were close to the Nernstian theoretical value of 0.059 V at 25°C . This model assumes that the number of protons was equal to the number of the transferred

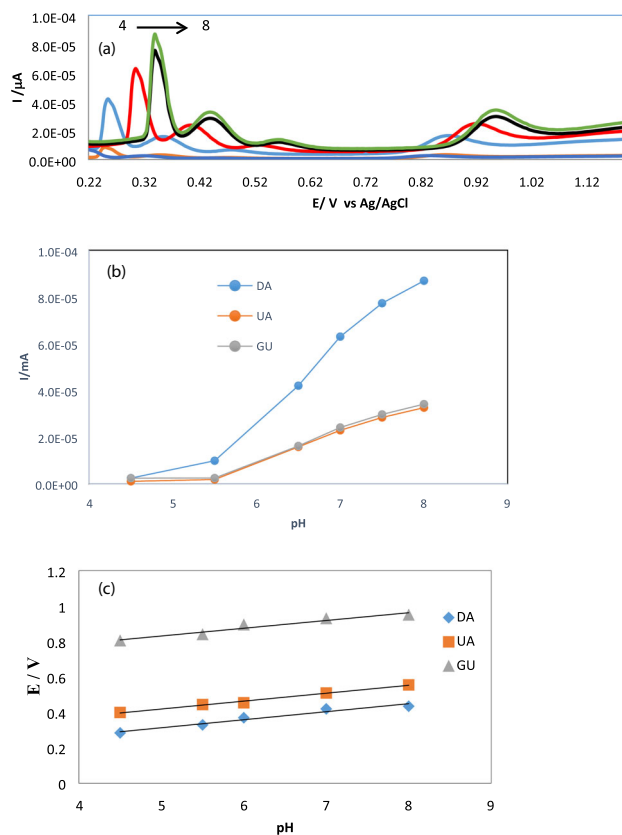


Fig. 7 a Effect of pH value on the electrochemistry behavior of $100 \mu\text{M}$ of analytes (color blue, red, black, and green for pH 4, 5, 7, and 8, respectively), b relationship between peak current and pH and c linear relationship between oxidation peak potential (E_{pa}) and pH at CM/SDS/AgNPs/MWCNT/GCE electrode

electrons in the electrochemical processes. According to the results, the electrochemical oxidation of guanine followed a loss of $4e^-$, while DA and UA followed loss of $2e^-$. The effects of various supporting electrolytes were also studied. The results showed that Na_2SO_4 , Na_2CO_3 , NaCl , and KNO_3 did not significantly enhanced the DPV peak currents. But the current in KCl solution increased and DPV peaks were separated better than other supporting electrolytes. Also, the background current is also the lowest in comparison to other electrolytes. The results show that DPV peak currents of analytes significantly increased after increasing concentration of KCl up to 0.1 mol L^{-1} and remain approximately constant at higher concentrations.

Therefore, a concentration of 0.1 mol L^{-1} of KCl was selected and applied for further studies. Herein, DA and UA electron transfer behavior was studied by changing the amount of silver nanoparticles in the GCE. The responses of GCE/MWCNTs surface electrodes containing different volumes of AgNPs were detected at pH 7 for 0.1 mol L^{-1} KCl solution. According to the results, increasing the number of the nanoparticle to $10 \mu\text{L}$ increases the DPV current. After adding $10 \mu\text{L}$ of AgNPs, there was little change in the amount of DPV currents. Therefore, the $10.0 \mu\text{L}$ volume of silver nanoparticles is suitable for reaching the highest sensitivity. The aggregation of AgNPs decreases the active surface area of nanoparticles and hence, remarkably decreases the AgNPs activities. Therefore, an experiment was performed using SDS to enhance the applicability and stabilization of AgNPs.

3.4 Investigation of scan rate

Beneficial information about the mechanism of electrochemical reactions usually can be achieved from the investigation of cyclic voltammetry at various scan rates. The effects of scan rate on the electrochemical signal of analytes were studied by a constructed composite using $10 \mu\text{M}$ of $\text{K}_3[\text{Fe}(\text{CN})_6]$ at optimum conditions. Figure 8a shows the influence of the scan rate on the cyclic voltammograms of analytes in the range of $40\text{--}150 \text{ mV s}^{-1}$. A dependence of i_p on $v^{1/2}$ and i_p and v for anodic peak corresponded to the following equations: $I_{p_a}(A) = 3.01v^{1/2} - 1.21$ ($R^2 = 0.995$) and $I_{p_a}(A) = 0.16v + 12.25$ ($R^2 = 0.986$) (Fig. 8b), respectively. The first equation is a typical diffusion-controlled

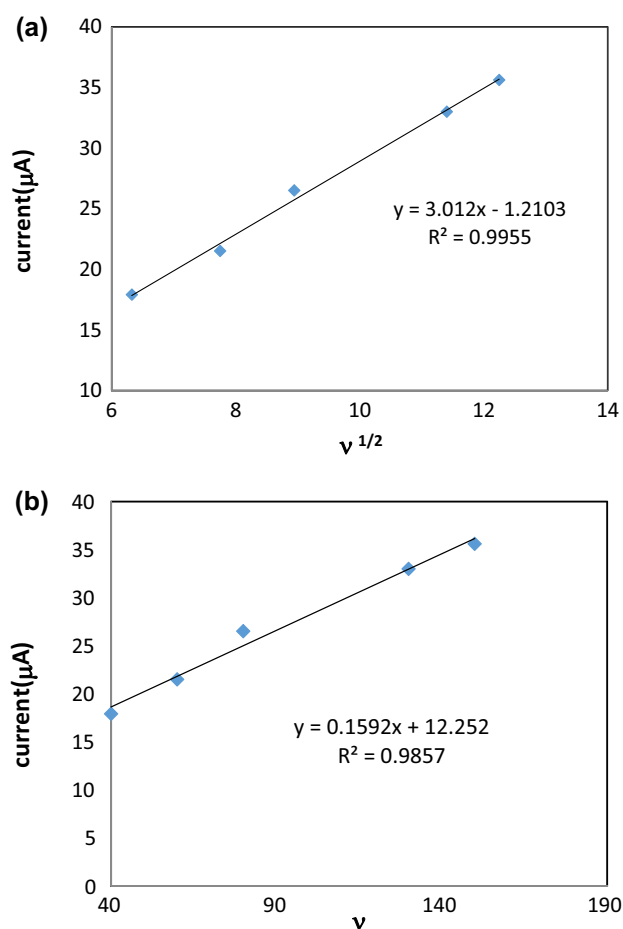


Fig. 8 a Influence of scan rate on anodic peak currents in the range of $40\text{--}150 \text{ mV s}^{-1}$ a dependence of i_p on $v^{1/2}$ and b dependence of i_p and v

reaction, whereas the second one is a redox reaction controlled by adsorption. These equations indicated a mixed adsorption–diffusion-controlled process.

3.5 Surface area study of nanocomposite

The effective surface of nanocomposite was evaluated by chronoamperometry of $\text{K}_3\text{Fe}(\text{CN})_6$. The graph of current as a function of time (I vs. $t^{-1/2}$) was considered. The linear plot reveals the Cottrellian behavior and diffusion of $\text{K}_3\text{Fe}(\text{CN})_6$ from bulk solution toward the electrode's surface. The slope of linear region of the Cottrell plot was used, and the diffusion coefficient of $\text{K}_3\text{Fe}(\text{CN})_6$ was estimated. The calculated value was $5.30 \times 10^{-6} \text{ cm}^2 \text{ s}^{-1}$, which is in well compliance with reported diffusion value of $\text{K}_3\text{Fe}(\text{CN})_6$. Moreover, the surface area of electrode was calculated using Cottrell equation. The obtained microscopic area of the modified electrode was

0.139 cm⁻², which is approximately twice as the value for MWCNT/CPE (0.0801 cm⁻²) [32].

3.6 Analytical features of the constructed composite

Under the optimized conditions, DPV of the different concentrations of analytes was recorded. The relationship between the i_{pa} and the concentration of DA, UA, and GU was tested on the surface of CM/AgNPs/SDS/MWCNT/GCE. Under the obtained optimum conditions, calibration plots were plotted. The obtained calibration equations, correlation coefficients, and limit of detection are given in Table 1. The results indicate that the system is very sensitive for determination of DA, UA, and GU.

The repeatability of the modified electrode was considered by repetitive recording of DPV signals at a fixed concentration of 100 μmol L⁻¹ for each analytes. The relative standard deviations (RSD) of peak currents intensity were 2.8, 1.1, and 4% for DA, UA, and GU, respectively. These data show the good repeatability of the modified GCE response. The storage stability studies of 100 μmol L⁻¹ of targets using modified electrode demonstrated that peak current did not change considerably over the first 23 days decreased by only about 5% after 30 days. The results of repeatability and stability indicate an excellent repetition ability and good long-term stability of modified electrode.

Table 1 Results of the recovery analysis of DA and UA spiked in urine and DOPADIC samples

Sample	Analyte	Added (μM)	Found (μM)	Recovery (%)
Urine	DA	0	0	–
		23.0	22.8	99.1
		50	50.22	100.4
	GA	0	0	–
		30	32.1	107
		50	53.4	106.8
DOPADIC	DA	0	0	–
		30.0	28.2	94.0
		96.0	101.8	106.0
Serum	DA	0	7.04	–
		19	25.7	98.2
		60	68.2	97.0
	GU	0	13.5	–
		3.5	17.2	105.7

3.7 Interference study

To evaluate the selectivity of the proposed method in the determination of DA, UA, and GU in the presence of AA, the influence of various foreign species on the determination of 10.0 μmol L⁻¹ of DA, UA, and GU was selected and thoroughly studied. The tolerance limit was taken as the maximum concentration of foreign substances that lead to an approximate relative error of 10 ± 10%, with results that are shown in Table 2. As evident in Table 2, many biological molecules do not interfere with their measurements, even at high concentrations (cysteine, lysine, tryptophan, and tyrosine). Additionally, ascorbic acid does not show any signal at the potential range of determination. Therefore, the designed composite has a great selectivity for the determination of low levels of analytes.

3.8 Applications of the method to real samples

The applicability of the proposed method was validated by determination of analytes in various blood, urine, serum, and dopamine ampoule samples.

3.8.1 Determination of UA in the urine sample

The prepared urine sample was used to determine the amount of UA by CM/AgNPS/SDS/GCE

Table 2 Influence of various foreign species on determination of DA, UA, and GU using functionalized nanocomposite by GCE

Species	Tolerance limits		
	GU	UA	DA
Lucien	1000	1000	2
Phenylalanine	50	50	50
Cysteine	1000	1000	1000
Tyrosine	400	1000	30
Tryptophan	1000	30	30
Aspartic acid	30	5	5
Acetaminophen	2	2	2

($3.0 \times 10^{-4} \pm 4.3 \times 10^{-5} \mu\text{mol L}^{-1}$) and correlated with the value obtained by standard addition method ($2.7 \times 10^{-4} \mu\text{mol L}^{-1}$). The results presented here show the average of three-time measurements \pm standard deviation of the replicates. The calculated value of student's t test (0.98) was lower than the critical value of t (4.30) at $p = 0.05$ for three determinations.

3.8.2 Determination of DA at DOPADIC ampoule

The dopadic ampoule was prepared for the evaluation of DA. Three measurements were performed, and the average of analysis was calculated based on these values. The amount of DA was obtained by the

proposed sensor, which was $5.8 \times 10^{-3} \pm 2.6 \times 10^{-4}$ (three-time measurements \pm standard deviation). The concentration of DA was obtained by the standard addition method as a reference method (5.4×10^{-3}). The student t test was applied to test the presence of statistically significant differences between the results. The calculated t value (2.18) was lower than the critical (table) value (4.30). According to these results, there is no significant difference in the mean value of analysis ($p = 0.05$).

3.8.3 Recovery tests

3.8.3.1 Determination of DA and UA in urine and dopadic ampoule sample The standard addition method was applied for the evaluation of DA and UA in the spiked samples (Table 2). Various amounts of DA and UA were added into the samples, and the values of spiked samples were calculated. The results of urine sample (Table 2) indicated that the current study showed good recoveries (94–107%). Besides, the concentration of DA and GU was obtained in DOPADIC ampoule samples. The recoveries of spiked samples are also collected in Table 2.

3.8.3.2 Determination of DA, UA, and GU in serum sample The applicability of the method was tested by determining DA, UA, and GU in spiked serum samples. Different concentrations of analytes were

Table 3 Characteristic comparison of some reported modified electrodes for the determination of analytes with proposed method

Electrode	Method	LDR ^a ($\mu\text{mol L}^{-1}$)			LOD ^b ($\mu\text{mol L}^{-1}$)			References
		DA	UA	GU	DA	UA	GU	
Pd-CNFs/CPE ^c	DPV	0.5–160	2–20	–	0.2	0.7	–	[7]
AuNPs@MoS ₂ /GCE ^d	DPV	0.05–30	50–40,000	–	0.05	10	–	[33]
PImox–GO/GCE ^e	DPV	12–278	3.6–249.6	3.3–103.3	0.63	0.59	0.48	[18]
PAA-MWNTs/GCE ^f	DPV	5–500	3–60	–	1.5	–	1.0	[28]
Ag-PMel/GCE ^g	DPV	0.1–50	0.1–50	0.1–50	0.01	0.1	0.008	[16]
CM/AgNPs/SDS/MWCNTs	DPV	2–120	6–184	4–160	1.43	3.72	1.9	Current work

^aLinear dynamic range

^bLimit of detection

^cPalladium nanoparticle-loaded carbon nanofiber

^dGold nanoparticle-decorated MoS₂-modified GCE

^eOveroxidized polyimidazole (PImox) and graphene oxide copolymer-modified electrode

^fPoly(acrylic acid) (PAA)-multiwalled carbon-nanotubes

^gAg/melamine monomer/glassy carbon electrode

added to the serum samples, and DPV signals were recorded. The calculated recovery values are summarized in Table 2. The data presented are the average of three determinations. The results explain that the proposed composite could be apply to the simultaneous determination of targets in real biological samples with satisfactory outcomes. The response characteristics of modified electrode were compared with reported methods for determination of DA, UA, and GU (see Table 3). These characteristics clarify that the nanocomposite provides better sensitivity, the limit of detection, linear range, and selectivity over most of the reported electrodes.

4 Conclusion

Overall, we have successfully designed and fabricated functionalized CM/AgNPs/SDS/MWCNTs nanocomposite using GCE for the simultaneous determination of DA, UA, and GU in the presence of AA. The results showed that SDS is a good stabilizer of AgNPs and MWCNTs. While MWCNTs maintained network-like structure, aggregation of silver nanoparticles was prevented and smaller nanoparticles were obtained. To the best of our knowledge, there is no prior report on the simultaneous measurement of targets in the presence of AA using GCE modified with the proposed modifiers, especially CM for stabilization and functionalization. The results demonstrated that the developed nanocomposite had great electrocatalytic activity toward biomolecules oxidation than other constructed electrodes and bare GCE. Furthermore, the study of potential-interfering substances demonstrated that the proposed method was free from the usual interfering compounds. Compared with the reported modified electrodes, the designed nanocomposite displayed effective performances of wider linear range and lower detection limit, which suggests this strategy for selective and sensitive determination of these components and demonstrates the main function of functionalized AgNPs.

Compliance with ethical standards

Conflict of interest The authors declare no conflict of interest.

References

1. X. Liu, L. Zhang, S. Wei, S. Chen, X. Ou, *Biosens. Bioelectr.* **572**, 32–238 (2014)
2. Z.H. Guangli, P. He, W. Feng, S.H. Ding, J. Chen, L. Li, H. He, S. Zhang, F. Dong, *J. Electroanal. Chem.* **760**, 24 (2016)
3. C.M.D. Schleicherl, E.S. Ford, D.A. Lacher, *Am. J. Clin. Nutr.* **90**, 1252–1263 (2009)
4. A. Salimi, H. Mamkhezri, R. Hallaj, *Talanta* **70**, 823 (2006)
5. R. Zhang, S.J. Lu, L.Y. Zhang, G. Chen, *J. Chromatogr. A* **1374**, 261 (2014)
6. B. Ferry, E.P. Gifu, I. Sandu, L. Denoroy, S. Parrot, *J. Chromatogr. B* **951**, 52 (2014)
7. M.R. Moghadam, S. Dadfarnia, A.M.H. Shabani, P. Shahbazikhah, *Anal. Biochem.* **410**, 289 (2011)
8. S.P. Qi, B. Zhao, H.Q. Tang, X.Q. Jiang, *Electrochim. Acta* **161**, 395 (2015)
9. M. Liu, Q. Chen, C.L. Lai, Y.Y. Zhang, J.H. Deng, H.T. Li, S.Z. Yao, *Biosens. Bioelectron.* **48**, 75 (2013)
10. Z.H. Xue, Y. Feng, H. Guo, C.H.A. Hu, M.I. Mohamed, J.X. Lu, *RSC Adv.* **4**, 5849 (2014)
11. D.P. Quan, D.P. Tuyen, T.D. Lam, P.T.N. Tram, N.H. Binh, P.H. Viet, *Colloids Surf. B. Biointerfaces* **88**, 764 (2011)
12. Y. Li, J. Du, J. Yang, D. Liu, X. Lu, *Colloids Surf. B* **9**, 32 (2012)
13. A. Rezaei, M. Abbasi Tarighat, Kh. Mohammadi, *J. Mater. Sci.: Mater. Electron.* **30**, 13347–13359 (2019)
14. D. Jia, J. Dai, H. Yuan, L. Lei, D. Xiao, *Talanta* **85**, 2344 (2011)
15. F. Yang, Q. Xie, H. Zhang, Sh. Yu, X. Zhang, Y. Shen, *Sens. Actuator B Chem.* **210**, 232 (2015)
16. H.B. Wang, H.D. Zhang, L.L. Xu, T. Gan, K.J. Huang, Y.M. Liu, *J. Solid State Electr.* **18**, 2435–2442 (2014)
17. H. Bagheri, N. Pajooheshpour, B. Jamali, S. AliHajian, H. Khoshshafar, *Microchem. J.* **131**, 120 (2017)
18. X. Liu, L. Zhang, S. Wei, S. Chen, X. Ou, Q. Lu, *Biosens. Bioelectron.* **572**, 32 (2014)
19. S. Shahrokhian, H. Zare-Mehrjardi, *Sens. Actuator B Chem.* **121**, 530 (2007)
20. J. Huang, Y. Liu, H. Hou, T. You, *Biosens. Bioelectron.* **24**, 632 (2008)
21. J.D. Bhawalkar, G.S. He, P.N. Prasad, *Rep. Prog. Phys.* **59**, 1041 (1996)
22. L. Zheng, J.F. Song, *Sens. Actuator B* **135**, 650 (2009)
23. K. Mavani, M. Shah, *Int. J. Eng. Res. Technol.* **2**, 1–5 (2013)
24. S. Tajbakhsh, K.H. Mohammadi, I. Deilami, K. Zandi, M. Fouladvand, E. Ramedani, G. Asayesh, *Afr. J. Biotechnol.* **7**, 3832 (2008)
25. M. Stucki, J.A. Clapperton, D. Mohammad, M.B. Yaffe, S.J. Smerdon, S.P. Jackson, *Cell* **123**, 1213 (2005)

26. P. Anand, A.B. Kunnumakkara, R.A. Newman, B.B. Aggarwal, *Mol. Pharm.* **4**, 807 (2007)
27. N. Sato, H. Okuma, *Sens. Actuat. B Chem.* **129**, 188 (2008)
28. A. Liu, I. Honma, H. Zhou, *Biosens. Bioelectron.* **23**, 74–80 (2007)
29. A. Afkahi, M. Abbasi-Tarighat, M. Bahram, H. Abdollahi, *Anal. Chim. Acta* **613**, 144 (2008)
30. D. Dastan, N. Chaure, M. Kartha, *J. Mater. Sci.: Mater. Electron.* **28**, 7784–7796 (2017)
31. D. Dastan, P.U. Londhe, N.B. Chaure, *J. Mater. Sci.: Mater. Electron.* **25**, 3473–3479 (2014)
32. J.E. Baur, R.M. Wightman, *J. Electroanal. Chem. Interfaces Electrochem.* **305**, 73–81 (1991)
33. H. Sun, J. Chao, X. Zuo, S. Su, X. Liu, L. Yuwen, C. Fan, L. Wang, *Rsc Adv.* **4**, 27625 (2014)

Publisher's Note Springer Nature remains neutral with regard to jurisdictional claims in published maps and institutional affiliations.